THE JOURNAL OF PHYSICAL CHEMISTRY Letters

Letter

pubs.acs.org/JPCL

Synthetic Conditions for High-Accuracy Size Control of PbS Quantum Dots

Jianbing Zhang,[†,‡] Ryan W. Crisp,[‡,§] Jianbo Gao,[‡,∥] Daniel M. Kroupa,[‡,⊥] Matthew C. Beard,[‡] and Joseph M. Luther*[,‡]

[†]School of Optical and Electronic Information, Huazhong University of Science and Technology, 1037 Luoyu Road, Wuhan, Hubei 430074, China

[‡]Chemical and Material Sciences Center, National Renewable Energy Laboratory, 15013 Denver West Parkway, Golden, Colorado 80401, United States

[§]Department of Physics, Colorado School of Mines, 1523 Illinois Street, Golden, Colorado 80401, United States

[∥]Center for Advanced Solar Photophysics, Los Alamos National Laboratory, Los Alamos, New Mexico 87545, United States

[⊥]Department of Chemistry and Biochemistry, University of Colorado, Boulder, Colorado 80309, United States

ABSTRACT: Decreasing the variability in quantum dot (QD) syntheses is desirable for better uniformity of samples for use in QD-based studies and applications. Here we report a highly reproducible linear relationship between the concentration of ligand (in this case oleic acid, OA) and the lowest energy exciton peak position (nm) of the resulting PbS QDs for various hot-injection temperatures. Thus, for a given injection temperature, the size of the PbS QD product is purely controlled by the amount of OA. We used this relationship to study PbS QD solar cells that are fabricated from the same size of PbS QDs but synthesized using four different injection temperatures: 95, 120, 150, and 185 °C. We find that the power conversion efficiency does not depend on injection temperature but that the V_{oc} is higher for QDs synthesized at lower temperatures while the J_{sc} is improved in higher temperature QDs.

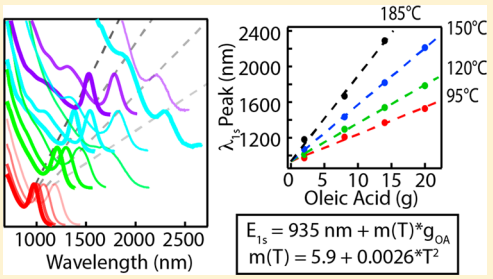

The appealing aspects of quantum dots (QDs) have led to their proliferation in numerous studies of solar cells,[1−4] light-emitting diodes,[5] infrared photodetectors,[6,7] and field effect transistors(FETs).[8] Such studies often require that the QD synthesis be an independent variable. At present, most PbS QDs are synthesized via a hot-injection method, with oleic acid (OA) as the chosen ligand due to the ease of size and size-dispersion control.[9] Furthermore, the popular Hines method produces PbS QDs free of reactant precursor residue.[10−13] With the Hines method, injection temperature, T_{inj}, the amount of sulfur precursor, reaction time, and the amount of free acid all affect the QD size (and the related first exciton peak position or bandgap). In general, more free acid, increased anion precursor amount, or higher T_{inj} leads to larger QDs.[14−19] Given these qualitative rules, accurately synthesizing a specific QD size requires systematically changing the amount of free acid or T_{inj}, often requiring a series of attempts to obtain the desired size. Similarly, accurately quenching a reaction at a given time is difficult. Such variability in QD synthesis inevitably leads to uncontrolled variations in resulting material and device characteristics and thus complicates studies intended to tease out differences due to, for example, device fabrication or film treatments within various applications. We develop a quantitative relationship between the OA concentration, [OA], and the resulting PbS QD size for different T_{inj}. The controlled synthetic procedure developed herein lowers the synthetic variability. To demonstrate how this relationship can be employed, we investigated how the performance of PbS QD solar cells varies with T_{inj} keeping the QD size constant. For this experiment, following the prescribed synthetic procedure required only one synthesis at each temperature to produce the required QD size.

We performed four syntheses varying the [OA] from $2g/V_{rxn}$ to $20g/V_{rxn}$ (where V_{rxn} is the total reaction volume) at each of four temperatures resulting in 16 syntheses (note that for the highest T_{inj} and largest [OA], the product QDs were too large and exhibited a large size distribution and thus were not further analyzed). Table 1 and Figure 1 summarize the results. In line with previous reports, the QD size increases with the amount of free acid relative to the cation precursor amount (see Figure 1a,b). In this work, we explicitly hold the cation precursor amount constant. We find that the lowest energy exciton peak position (wavelength of the 1S exciton, λ_{1S}) , and the OA amount exhibit a linear relationship whose slope depends on T_{inj} (Figure 1b). The higher T_{inj}, the larger the QDs that can be obtained, indicated by the steeper slope. We derived a general relationship that defines λ_{1S} to the grams of OA, g_{OA}/V_{rxn}, and T_{inj} given by

Received: April 2, 2015
Accepted: April 30, 2015
Published: April 30, 2015

DOI: 10.1021/acs.jpclett.5b00689
J. Phys. Chem. Lett. 2015, 6, 1830−1833

Table 1. Results of PbS QDs Synthesized at Different Injection Temperatures with Various OA Amounts[a]

		OA			
		2*g*	8*g*	14*g*	20*g*
95 °C	1st exciton peak (nm)	973	1208	1369	1528
	size (nm)	3.2	4.2	4.9	5.8
	particle (μmol)	3.45	1.41	0.84	0.57
	chemical yield (%)	84.4 ± 8	93.8 ± 9	96.7 ± 10	103.8 ± 10
	size dispersion (%)	5.7	5.8	4.8	4.8
120 °C	1st exciton peak (nm)	1011	1296	1540	1785
	size (nm)	3.3	4.6	5.9	7.5
	particle (μmol)	2.57	0.97	0.46	0.19
	chemical yield (%)	77.1 ± 8	89.2 ± 9	89.4 ± 9	73.7 ± 7
	size dispersion (%)	6.3	6.8	5.7	5.9
150 °C	1st exciton peak (nm)	1070	1434	1818	2212
	size (nm)	3.6	5.3	7.7	11.6
	particle (μmol)	2.12	0.59	0.18	0.074
	chemical yield (%)	83.3 ± 8	82.8 ± 8	80 ± 8	109 ± 11
	size dispersion (%)	7.1	8.3	7.8	9
185 °C	1st exciton peak (nm)	1181	1668	2290	
	size (nm)	4.1	6.7	12.6	
	particle (μmol)	1.37	0.28	0.045	
	chemical yield (%)	85.4 ± 9	80 ± 8	87.4 ± 9	
	size dispersion (%)	7.3	11.8	10.2	

[a]See the characterization section for details of determination of sample properties.

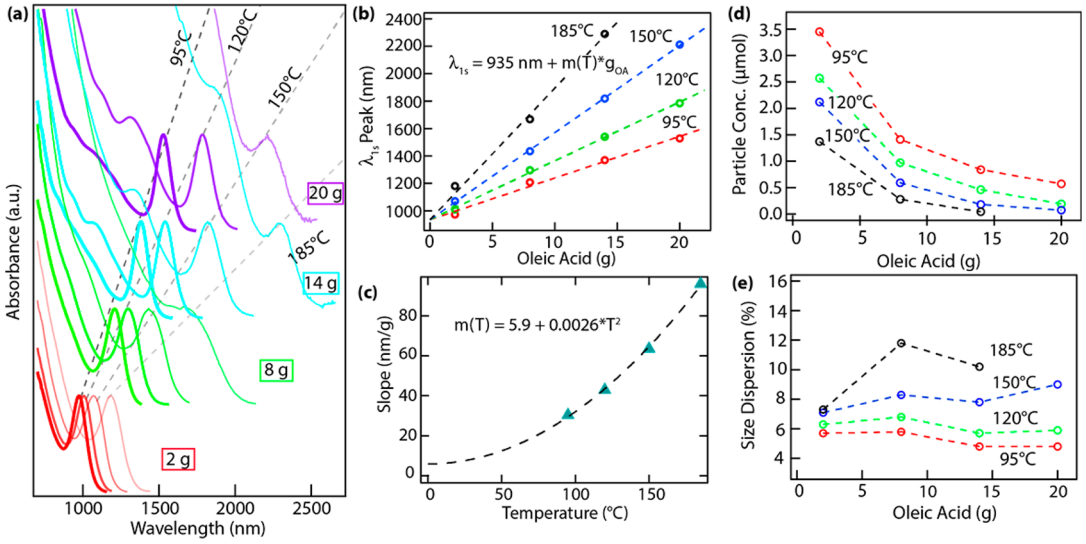

Figure 1. (a) Absorption spectra of PbS QDs synthesized at different injection temperatures with various OA amounts. Red traces are for synthesis with 2 g of OA, green are for 8 g, blue are for 14 g, and purple traces are for 20 g OA. The injection temperature was varied from 95 to 185 °C (the different injection temperatures have faded colors). (b) The peak of the 1S exciton as a function of grams of OA. The traces are a best-fit linear function, and the slope is plotted versus temperature in panel c. (d) Particle concentration as a function of the amount of OA added. (e) Size dispersion (%).

$$\lambda_{1S} = 935nm + m(T_{inj})\cdot g_{OA} \quad (1)$$

where $m(T_{inj}) = 5.9 + 0.0026\cdot T_{inj}^2$ is the temperature-dependent slope as shown in Figure 1c. We denote the g_{OA} rather than [OA] because it is a more useful experimental parameter, while [OA] can easily be determined from the synthetic parameters.

The dependence of QD size on [OA] is consistent with studies by Abe et al.,[20] which demonstrated that free acid does not change the reaction rate but instead increases the monomer solubility. Monomers are consumed by either QD growth or nucleation. Increasing the monomer solubility pushes the consumption toward growth rather than nucleation. As a result, fewer nanoparticles are formed, leading to more QD growth and larger QD sizes with the reaction rate remaining fixed. This concept is captured in our data (Figure 1d) where we observe a larger particle concentration for smaller [OA], resulting in smaller QDs (lower λ_{1S}). This temperature dependence is also consistent with PbSe QDs syntheses.[19]

All of the syntheses have chemical yields above ~80% (Table 1), and the yield does not display any systematic dependence on either T_{inj} or [OA]. Figure 1e shows the size dispersions of the PbS QDs synthesized under different conditions. Apparently, lower T_{inj} and higher [OA] leads to narrower size dispersion (the case of 20 g OA at 150 °C is an outlier).

DOI: 10.1021/acs.jpclett.5b00689
J. Phys. Chem. Lett. 2015, 6, 1830−1833

Because the syntheses at different conditions have similar chemical yield, lower T_{inj} and higher [OA] are desirable to achieve better size dispersion. Size focusing has been shown to occur with higher monomer concentration.[11] Equation 1 implies that the minimum λ_{1S} that can be achieved using this protocol is 935 nm. To achieve a lower λ_{1S} (smaller QDs) there are at least two exceptions to eq 1: (1) the linearity between OA concentration and λ_{1S} breaks down for the lowest injection temperature, T_{inj} = 95 °C, when [OA] is less than $2g/V_{rxn}$ and we can consistently achieve λ_{1S} of ∼870 nm using smaller amounts of OA. (2) To achieve even smaller λ_{1S} the reaction can be quenched at earlier times, arresting the growth at the expense of lower chemical yields. We have used this strategy to achieve PbS QD samples with λ_{1S} as low as 633 nm.[21]

Using eq 1, we synthesized PbS QDs with λ_{1S} at 1145 nm (1.08 eV) at four different T_{inj} (Figure 2a). The OA amounts

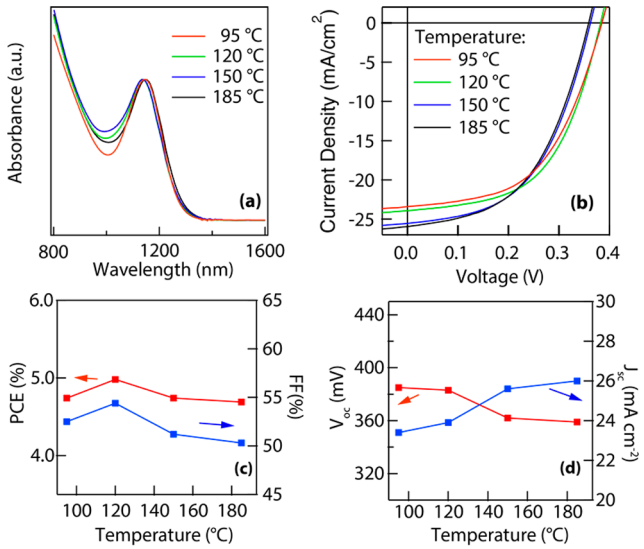

Figure 2. (a) Absorption spectra of four different syntheses with λ_{1S} of 1145 nm. (b) $J-V$ characteristics of the four PbS QD solar cells. (c) Variation in the power conversion efficiency (PCE) and FF and (d) V_{oc} and J_{sc} as a function of injection temperature.

used were approximately 7.9, 5.5, 3.8, and 2.2 g for 95, 120, 150, and 185 °C, respectively. The resulting PbS QDs have λ_{1S} that achieved the targeted value to within ±10 nm, confirming eq 1.

Solar cells utilized a TiO_2/PbS heterojunction structure and PbI_2 ligand exchange procedure described by Crisp et al.[22] with details provided later. The $J-V$ characteristics of the devices (Figure 2b) display a power conversion efficiency that fluctuates between ∼4.7 and ∼5% (Figure 2c). The V_{oc} decreases as T_{inj} increases, while the J_{sc} increases (Figure 2d). The T_{inj} could impact the quality of the resulting QDs by better expelling impurities (i.e., creating fewer vacancies) at higher T_{inj}, impacting surface defect formation, and impacting QD shape. A QD solid with fewer defective QDs should result in a higher V_{oc}, but higher V_{oc} values in this work are observed at lower T_{inj}. The size dispersion, however, does improve for lower T_{inj} (Figure 1e) and could be responsible for the higher V_{oc}. Other processes such as the purification procedure and growth rate may affect the device performance but are held constant here.[23,24]

In conclusion, a linear relationship between the λ_{1S} and the OA amount was discovered for the PbS QD synthesis, providing an accurate size control procedure. For a given T_{inj}, the QD size increases while the number of particles decreases with increasing OA amounts. Similarly, for a given OA amount, the QD size increases while the number of particles decreases with increasing T_{inj}. In terms of size dispersion, lower temperature and higher [OA] are favorable. Solar cells made from the same size PbS QDs synthesized at different conditions demonstrate similar power conversion efficiency, but the V_{oc} decreases for higher T_{inj} while the J_{sc} increases.

METHODS

Chemicals. Lead oxide (PbO, 99.99%) was purchased from Alfa Aesar, bis(trimethylsilyl) sulfide ($(TMS)_2S$, synthesis grade), oleic acid (OA, tech. grade, 90%), acetonitrile (ACN, anhydrous, 99.8%), tetrachloroethylene (TCE, ≥99.9%), hexane (≥95%), ethanol (≥99.5%), lead(II) iodide (PbI_2), 3-mercatopropionic acid (MPA), methanol, and *N*,*N*-dimethylformamide (DMF) were purchased from Aldrich. All chemicals were used as received.

Synthesis of PbS QDs. The PbS QDs were synthesized following a modification of the Hines method.[9] In a typical synthesis, 0.45 g PbO, 2−20 g OA, and 10 g ODE were loaded in a 100 mL flask and heated to 110 °C for 20 min under vacuum to obtain a clear solution. The temperature was adjusted to the desired injection temperature (95−185 °C) followed by a fast injection of 210 μL of $(TMS)_2S$ diluted in 5 mL of ODE. Immediately before injection, the heating mantle was removed and the solution cooled naturally after the injection. When the reaction solution reached 30 °C, 30 μL of raw solution was removed and dissolved in 2.5 mL of TCE for absorption measurements. Before device fabrication, the PbS QDs were purified twice using hexane and ethanol and redispersed in octane at a concentration of 40 mg/mL.

Solar Cell Fabrication. QD solar cells consisting of ITO/TiO_2/PbS QDs/MoO_3/Al were fabricated following our previous report.[22] Multiple coatings of PbS QDs were spin-coated at 1000 rpm in ambient atmosphere from a 40 mg/mL solution of PbS QDs in octane. After each coating, the device was soaked in 10 mM PbI_2 in DMF for ∼2 min and rinsed in ACN. Four layers of PbI_2-treated QDs were followed by two more QD layers that were briefly dipped in 10% MPA in methanol and rinsed with methanol instead of ACN. The devices were annealed at 110 °C in a N_2-filled glovebox for 20 min. The top electrodes, a 20 nm molybdenum trioxide layer, and 150 nm Al layer were thermally evaporated at a rate of 0.3 and 15 Å/s, respectively.

Characterization. Optical absorption spectra were collected using a Shimadzu UV-3600 spectrophotometer. The QD size (d) was determined from λ_{1S} using the sizing curve given by Moreels et al., and the QD sample concentration was determined from Beer's Law using the QD size-independent extinction coefficient at 400 nm also described by Moreels et al.[25] The Pb/S ratios (R) of PbS QDs with different sizes were derived from the data reported by Jeong.[26] The number of S atoms per QD (S_{QD}) was calculated by $S_{QD} = (4\pi/3)\cdot(d/a)^3\cdot(1/(1+R))$, where R is the Pb/S ratio, d is the dot size, and bulk lattice constant, a, is 0.59 nm. The chemical yield for a synthesis was calculated based on particle number and S_{QD}. The size dispersion was estimated by fitting the absorption spectra following our previous procedure.[11] For device characterization, current and voltage characteristics ($J-V$) curves were acquired in a glovebox using a Newport solar simulator with the intensity

DOI: 10.1021/acs.jpclett.5b00689
J. Phys. Chem. Lett. 2015, 6, 1830−1833

set to match the AM1.5 spectrum by measuring the current output of a calibrated Si photodiode.

AUTHOR INFORMATION

Corresponding Author

*E-mail: joey.luther@nrel.gov.

Notes

The authors declare no competing financial interest.

ACKNOWLEDGMENTS

This work was supported by the U.S. Department of Energy, Office of Science, Office of Basic Energy Sciences. The concept, analysis, and manuscript development were derived in and supported as part of the Center for Advanced Solar Photophysics within the Energy Frontier Research Centers program. Quantum dot synthesis was provided by the Solar Photochemistry program within the Division of Chemical Sciences, Geosciences and Biosciences division. Solar cell fabrication was supported by the U.S. Department of Energy Sunshot program. DOE funding was provided to NREL through contract DE-AC36-08G028308.

REFERENCES

(1) Luther, J. M.; Law, M.; Beard, M. C.; Song, Q.; Reese, M. O.; Ellingson, R. J.; Nozik, A. J. Schottky Solar Cells Based on Colloidal Nanocrystal Films. *Nano Lett.* **2008**, *8*, 3488−3492.

(2) Koleilat, G. I.; Levina, L.; Shukla, H.; Myrskog, S. H.; Hinds, S.; Pattantyus-Abraham, A. G.; Sargent, E. H. Efficient, Stable Infrared Photovoltaics Based on Solution-Cast Colloidal Quantum Dots. *ACS Nano* **2008**, *2*, 833−840.

(3) Zhao, N.; Osedach, T. P.; Chang, L.-Y.; Geyer, S. M.; Wanger, D.; Binda, M. T.; Arango, A. C.; Bawendi, M. G.; Bulovic, V. Colloidal PbS Quantum Dot Solar Cells with High Fill Factor. *ACS Nano* **2010**, *4*, 3743−3752.

(4) Kim, M. R.; Ma, D. Quantum-Dot-Based Solar Cells: Recent Advances, Strategies, and Challenges. *J. Phys. Chem. Lett.* **2015**, *6*, 85−99.

(5) Sun, L.; Choi, J. J.; Stachnik, D.; Bartnik, A. C.; Hyun, B.-R.; Malliaras, G. G.; Hanrath, T.; Wise, F. W. Bright Infrared Quantum-Dot Light-Emitting Diodes Through Inter-Dot Spacing Control. *Nat. Nanotechnol.* **2012**, *7*, 369−373.

(6) Konstantatos, G.; Howard, I.; Fischer, A.; Hoogland, S.; Clifford, J.; Klem, E.; Levina, L.; Sargent, E. H. Ultrasensitive Solution-Cast Quantum Dot Photodetectors. *Nature* **2006**, *442*, 180−183.

(7) Sukhovatkin, V.; Hinds, S.; Brzozowski, L.; Sargent, E. H. Colloidal Quantum-Dot Photodetectors Exploiting Multiexciton Generation. *Science* **2009**, *324*, 1542−1544.

(8) Talapin, D. V.; Lee, J. S.; Kovalenko, M. V.; Shevchenko, E. V. Prospects of Colloidal Nanocrystals for Electronic and Optoelectronic Applications. *Chem. Rev.* **2010**, *110*, 389−458.

(9) Hines, M. A.; Scholes, G. D. Colloidal PbS Nanocrystals with Size-Tunable Near-Infrared Emission: Observation of Post-Synthesis Self-Narrowing of the Particle Size Distribution. *Adv. Mater.* **2003**, *15*, 1844−1849.

(10) Moreels, I.; Justo, Y.; De Geyter, B.; Haustraete, K.; Martins, J. C.; Hens, Z. Size-Tunable, Bright, and Stable PbS Quantum Dots: A Surface Chemistry Study. *ACS Nano* **2011**, *5*, 2004−2012.

(11) Zhang, J.; Gao, J.; Miller, E. M.; Luther, J. M.; Beard, M. C. Diffusion-Controlled Synthesis of PbS and PbSe Quantum Dots with in Situ Halide Passivation for Quantum Dot Solar Cells. *ACS Nano* **2014**, *8*, 614−622.

(12) Cademartiri, L.; Bertolotti, J.; Sapienza, R.; Wiersma, D. S.; von Freymann, G.; Ozin, G. A. Multigram Scale, Solventless, and Diffusion-Controlled Route to Highly Monodisperse PbS Nanocrystals. *J. Phys. Chem. B* **2006**, *110*, 671−673.

(13) Yuan, M.; Kemp, K. W.; Thon, S. M.; Kim, J. Y.; Chou, K. W.; Amassian, A.; Sargent, E. H. High-Performance Quantum-Dot Solids via Elemental Sulfur Synthesis. *Adv. Mater.* **2014**, *26*, 3513−3519.

(14) Yu, W. W.; Peng, X. Formation of High-Quality CdS and Other II−VI Semiconductor Nanocrystals in Noncoordinating Solvents: Tunable Reactivity of Monomers. *Angew. Chem., Int. Ed.* **2002**, *41*, 2368−2371.

(15) Bullen, C. R.; Mulvaney, P. Nucleation and Growth Kinetics of CdSe Nanocrystals in Octadecene. *Nano Lett.* **2004**, *4*, 2303−2307.

(16) Battaglia, D.; Peng, X. Formation of High Quality InP and InAs Nanocrystals in a Noncoordinating Solvent. *Nano Lett.* **2002**, *2*, 1027−1030.

(17) Dai, Q.; Kan, S.; Li, D.; Jiang, S.; Chen, H.; Zhang, M.; Gao, S.; Nie, Y.; Lu, H.; Qu, Q.; Zou, G. Effect of Ligands and Growth Temperature on the Growth Kinetics and Crystal Size of Colloidal CdSe Nanocrystals. *Mater. Lett.* **2006**, *60*, 2925−2928.

(18) Zhang, J.; Zhang, D. Photoluminescence and Growth Kinetics of High-Quality Indium Arsenide and InAs-Based Core/Shell Colloidal Nanocrystals Synthesized Using Arsine (AsH_3) Generated via Zinc Arsenide as the Arsenic Source. *Chem. Mater.* **2010**, *22*, 1579−1584.

(19) Joo, J.; Pietryga, J. M.; McGuire, J. A.; Jeon, S. H.; Williams, D. J.; Wang, H. L.; Klimov, V. I. A Reduction Pathway in the Synthesis of PbSe Nanocrystal Quantum Dots. *J. Am. Chem. Soc.* **2009**, *131*, 10620−10628.

(20) Abe, S.; Capek, R. K.; De Geyter, B.; Hens, Z. Reaction Chemistry/Nanocrystal Property Relations in the Hot Injection Synthesis, the Role of the Solute Solubility. *ACS Nano* **2013**, *7*, 943−949.

(21) Erslev, P. T.; Chen, H. Y.; Gao, J. B.; Beard, M. C.; Frank, A. J.; van de Lagemaat, J.; Johnson, J. C.; Luther, J. M. Sharp Exponential Band Tails in Highly Disordered Lead Sulfide Quantum Dot Arrays. *Phys. Rev. B* **2012**, *86*, 155313.

(22) Crisp, R. W.; Kroupa, D. M.; Marshall, A. R.; Miller, E. M.; Zhang, J.; Beard, M. C.; Luther, J. M. Metal Halide Solid-State Surface Treatment for High Efficiency PbS and PbSe QD Solar Cells. *Sci. Rep.* **2015**, *5*, 9945.

(23) Fu, H.; Tsang, S.-W.; Zhang, Y.; Ouyang, J.; Lu, J.; Yu, K.; Tao, Y. Impact of the Growth Conditions of Colloidal PbS Nanocrystals on Photovoltaic Device Performance. *Chem. Mater.* **2011**, *23*, 1805−1810.

(24) Hassinen, A.; Moreels, I.; De Nolf, K.; Smet, P. F.; Martins, J. C.; Hens, Z. Short-Chain Alcohols Strip X-Type Ligands and Quench the Luminescence of PbSe and CdSe Quantum Dots, Acetonitrile Does Not. *J. Am. Chem. Soc.* **2012**, *134*, 20705−20712.

(25) Moreels, I.; Lambert, K.; Smeets, D.; De Muynck, D.; Nollet, T.; Martins, J. C.; Vanhaecke, F.; Vantomme, A.; Delerue, C.; Allan, G.; Hens, Z. Size-Dependent Optical Properties of Colloidal PbS Quantum Dots. *ACS Nano* **2009**, *3*, 3023−3030.

(26) Choi, H.; Ko, J.-H.; Kim, Y.-H.; Jeong, S. Steric-Hindrance-Driven Shape Transition in PbS Quantum Dots: Understanding Size-Dependent Stability. *J. Am. Chem. Soc.* **2013**, *135*, 5278−5281.

DOI: 10.1021/acs.jpclett.5b00689
J. Phys. Chem. Lett. 2015, 6, 1830−1833